GFZ

Helmholtz Centre
POTSDAM

HELMHOLTZ CENTRE POTSDAM
GFZ GERMAN RESEARCH CENTRE
FOR GEOSCIENCES

Frederik Tilmann, Xiaohui Yuan, Georg Rümpker, Elisa Rindraharisaona

ZE 2012-2014

SELASOMA Project, Madagascar 2012-2014

Scientific Technical Report STR - Data 17/06

www.gfz-potsdam.de

HELMHOLTZ
ASSOCIATION

Recommended citation for the data report:

Tilmann, F., Yuan, X., Rümpker, G., Rindraharisaona, E. (2017). ZE 2012-2014: SELASOMA Project, Madagascar 2012-2014 (p.). GFZ German Research Centre for Geosciences. https://doi.org/10.2312/gfz.b103-17061

If you use the dataset described in this report, please use the following citation:

Tilmann, F., Yuan, X., Rümpker, G., Rindraharisaona, E. (n.d.). SELASOMA Project, Madagascar 2012-2014. Deutsches GeoForschungsZentrum GFZ. https://doi.org/10.14470/mr7567431421

The raw unprocessed data from cube data loggers and logfiles from EDL stations are archived as assembled dataset and should be cited as:

Tilmann, F., Yuan, X., Rümpker, G., Rindraharisaona, E. (2017). Supplementary data for SELASOMA Project, Madagascar 2012-2014 - Datasets [Data set]. GFZ Data Services. https://doi.org/10.5880/gipp.201204.1

Imprint

Helmholtz Centre Potsdam
GFZ German Research Centre for Geosciences

Telegrafenberg
D-14473 Potsdam

Published in Potsdam, Germany
December 2017

ISSN 2190-7110

DOI: 10.2312/GFZ.b103-17061
URN: urn:nbn:de:kobv:b103-17061

This work is published in the GFZ series
Scientific Technical Report (STR)
and electronically available at GFZ website
www.gfz-potsdam.de

Frederik Tilmann[1], Xiaohui Yuan[1], Georg Rümpker[2], Elisa Rindraharisaona[3]

ZE 2012-2014

SELASOMA Project, Madagascar 2012-2014

[1] GFZ German Research Centre for Geosciences, Potsdam

[2] Goethe-Universität Frankfurt

[3] Institute and Observatory of Geophysics in Antananarivo - IOGA, GFZ German Research Centre for Geosciences

Scientific Technical Report STR - Data 17/06

Abstract

The island of Madagascar occupies a key region in both the assembly and the multi-stage breakup of Gondwanaland, itself part of the super-continent Pangaea. Madagascar consists of an amalgamation of continental material with the oldest rocks being of Archaean age. Its ancient fabric is characterised by several shear zones, some of them running oblique to the N-S trend, in particular in the south of the island. More recently during the Neogene, moderate volcanism has occurred in the Central and Northern part of the island, and there are indications of uplift throughout Eastern Madagascar over the last 10 Ma. Although Madagascar is now located within the interior of the African plate and far away from major plate boundaries (>1000 km from the East African rift system and even further from the Central and South-West Indian Ridges), its seismic activity indicates that some deformation is taking place, and present-day kinematic models based on geodetic data and earthquake moment tensors in the global catalogues identify a diffuse N-S-oriented minor boundary separating two microplates, which appears to pass through Madagascar. In spite of the presence of Archaean and Proterozoic rocks continent-wide scale studies indicate a thin lithosphere (<120 km) throughout Madagascar, but are based on sparse data and cannot resolve the difference between eastern and western Madagascar. We have operated an ENE-WSW oriented linear array of 25 broadband stations in southern Madagascar, extending from coast to coast and sampling the sedimentary basins in the west as well as the metamorphic rocks in the East, cutting geological boundaries seen at the surface at high angle. The array crosses the prominent Bongolava-Ranotsara shear zone which is thought to have been formed during Gondwanaland assembly. The array recorded the magnitude 5.3 earthquake of January 25, 2013 which occurred just off its western edge. In addition, in May 2013 we have deployed 25 short period sensors in the eastern part of the study area, where there is some so-far poorly characterised seismicity.

1 Data Acquisition

1.1 Experimental Design and instrumentation

The station distribution is shown in Fig. 1 and Table 1 summarises the most important information about each station.

Three different types of instruments were used in this experiment. The main profile had a nominal average station spacing of 17 km and was equipped EDL dataloggers and mostly CMG-3ESPs sensors. A few Trillium 240s were approximately equally spaced throughout the array. The power to these stations was supplied by solar panels. The permanent GEOFON station VOI forms an integral part of the array, and no temporary station was deployed in the immediate neighbourhood.

The areal array comprises Cube data loggers and Mark L4C 1 Hz sensors. These stations ran off batteries without recharging.

1.2 Site Descriptions and Possible Noise Sources

Stations were deployed in rural settings, mostly on the properties of individual land owners, or near schoolbuilding (see e.g. Fig. 2)

1.3 Sensor orientation

All stations were oriented along magnetic north. The declination at the location of station MS13 approximately at the centre of the array at the time of deployment (May 11, 2012) was 19° 19' W, changing by 1'/year in west direction) (Source: http://www.ngdc.noaa.gov/geomag-web/#declination). The azimuth of the nominal North components is thus ~341°. This value is recorded in the station metadata information in the GEOFON database; the variation of the magnetic field through Madagascar has not been taken into account, though, but should be small compared to the random orientation error.

2 Data Description

2.1 Data Completeness

An overview of instrument uptimes is given in Fig. 3. A relatively large amount of data was lost due to vandalism ranging from loss of power because of theft of the solar panels due to complete loss of data loggers. Some data was lost to technical issues, probably related to high humidity at selected station sites. A recurring problem were GPS gaps at a few of the Cube stations.

The security issues made it necessary to relocate some of the stations (MS06 and MS18, MS25 and AM16) and change the sensor type mid-experiment at some others (MS01, MS02, MS03, MS17, MS25).

2.2 Data Processing

The Cube data were converted to miniseed format using the *c2m* code written by Trond Ryberg (http://www.gfz-potsdam.de/en/section/geophysical-deep-sounding/infrastructure/geophysical-instrument-pool-potsdam-gipp/instruments/seismic-pool/recorder-dss-cube/) This code interpolates linearly between the raw data samples in order to ensure an even sampling rate of the output file. It assumes a linear drift between GPS fixes, when GPS reception is temporarily lost.

2.3 Noise Estimation

Fig. 7 shows noise probability density functions for all channels.

2.4 Timing Accuracy

An overview of the timing accuracy is given for the broadband stations in Fig. 4 - Fig. 6. In spite of a large number of gaps without GPS for station MS09, MS24 and other stations, particularly in 2014, the timing is thought to be correct for this station for standard seismological purposes.

However, based on inspections of the symmetry of the noise-correlation day stacks, the timing for station MS05 was found to be off by 60~s between 02/10/2012 and 05/02/2013, such that the indicated time is delayed with respect to the real time (equivalently seismic traces are apparently shifted to earlier time). Data recorded in the period from 12/07/2012 to 29/09/2012 and from 06/02/2013 to 28/04/2013 only showed noise with no discernible seismic signals or ambient displacement noise.

There is no indication in the log files of any problem. Such errant behaviour in the EDL is rare but a known phenomenon (T. Ryberg, pers. comm.). The timing of data in the GEOFON database was corrected for the indicated time period and the bad data removed but it still appears on the noise power density plots for station MS05 (Fig. Fig. 7).

The following short period stations had no GPS at the time of service, and last GPS fix was more than 2 days in the past. The time after the last GPS fix cannot be corrected, and absolute timing information should not be used between the last fix and indicated station service time; expected daily drift is up to ~10 ms/day *[RYBERG14]*

Station	Last fix	Service
AM04	2013-05-09	2013-11-02
AM11	2013-10-26	2013-10-31
AM12	2013-10-27	2013-11-01
AM17	2013-10-30	2013-11-05
AM20	2014-01-01	2014-05-15
MS25A	2013-05-10	2013-09-13

The following short period stations had gaps in excess of 20 days, but a linear correction through the gap could be carried out. Timing errors will be largest in the centre of the gap. The values given in the last column represent these expected and maximum 'largest errors' based on the statistical distribution of cube sensors during an experiment in Namibia *[RYBERG14]*. Gaps shorter than 20 days had expected errors of 5 ms and errors never exceeded 20 ms. No data exist on the likely timing errors beyond 40 days. Actual errors encountered in the Madagascar experiment might differ.

Station	Start gap	End gap	Gap days	Expected/max (ms)
AM01	2013-11-25	2013-12-28	33	13/36
	2014-01-13	2014-05-10	117	unreliable
AM12	2013-11-23	2013-12-18	25	8/27
	2014-01-28	2014-02-20	23	7/26
	2014-02-20	2014-04-26	65	unreliable
AM16A	2014-01-12	2014-02-11	30	16/40

3 Data Access

3.1 File format and access tools

The data are stored in the GEOFON database, and selected time windows can be requested by EIDA access tools as documented on http://geofon.gfz-potsdam.de/waveform/ . Normally the data are delivered in miniseed format. The current data access possibilities can always be found by resolving the DOI of the dataset.

3.2 Availability

The data are embargoed until May 2018.

4 Acknowledgements

We thank Prof. Gérard Rambolamana (Institute and Observatory of Geophysics in Antananarivo - IOGA) for supporting this initiative and letting us use storage space at the institute and Mirana Rakotoarisoa for various support in particular related to shipping and custom clearance. Andriamiranto Raveloson helped to set up this collaboration and helped with the organisation. Martina Gassenmeier, Michael Gummert, Ben Heit, Miriam Reiss, Felix Schneider, Ingo Wölbern, Rasoanaivo Christo, Rabeatoandro Johnson, and Andrianaivoarisoa Jean Bernardo are thanked for supporting the fieldwork. We also thank landowners in Madagascar for hosting our stations, and the Isalo Ranch lodge for providing intermediate storage space.

The funding for this experiment was provided by the expedition fund of the GFZ. Analysis of the data is funded by the DFG. The data are additionally being used in the context of a DAAD sponsored postdoctoral fellowhip to one of us (E. R.). Most of the instrumentation was provided by the GIPP (Geophysical Instrument Pool Potsdam); the University of Potsdam loaned us solar panels.

Table 1: Station table. Note that start and end times represent the maximum validity of the corresponding configurations, not the actual data availability or time in the field. Azi: Azimuth of north or '1' component.

Label	Lat	Lon	Ele	Azi	Rate	Sensor	ID	Logger	Id	Start	End	Channels
AM01	-21.07725	48.23924	43	341	50	L4-3D	3055	CUBE	725	2013-04-29	2014-12-31	HHZ HHN HHE
AM02	-21.24409	48.34717	11	341	50	L4-3D	1825	CUBE	727	2013-05-08	2014-12-31	HHZ HHN HHE
AM04	-21.18114	47.63818	454	341	50	L4-3D	3053	CUBE	728	2013-05-07	2014-12-31	HHZ HHN HHE
AM05	-21.17286	48.07654	45	341	50	L4-3D	4180	CUBE	625	2013-05-08	2014-12-31	HHZ HHN HHE
AM06	-21.04612	47.20041	1236	341	50	L4-3D	4191	CUBE	622	2013-05-06	2014-12-31	HHZ HHN HHE
AM07	-20.79577	47.17765	1817	341	50	L4-3D	4190	CUBE	620	2013-05-06	2014-12-31	HHZ HHN HHE
AM08	-21.32468	46.93855	1118	341	50	L4-3D	400290	CUBE	732	2013-05-04	2014-12-31	HHZ HHN HHE
AM09	-21.5598	47.51704	402	341	50	L4-3D	400288	CUBE	729	2013-05-06	2014-12-31	HHZ HHN HHE
AM10	-21.58659	47.96592	63	341	50	L4-3D	4182	CUBE	624	2013-05-07	2014-12-31	HHZ HHN HHE
AM11	-21.74314	47.49369	230	341	50	L4-3D	4201	CUBE	730	2013-05-06	2014-12-31	HHZ HHN HHE
AM12	-21.81696	47.87929	32	341	50	L4-3D	4188	CUBE	623	2013-05-07	2014-12-31	HHZ HHN HHE
AM13	-21.61401	46.8444	1010	341	50	L4-3D	4183	CUBE	626	2013-05-04	2014-12-31	HHZ HHN HHE
AM14	-22.52423	46.73701	647	341	50	L4-3D	4195	CUBE	735	2013-05-02	2014-12-31	HHZ HHN HHE
AM15	-22.05455	47.05158	1056	341	50	L4-3D	4200	CUBE	621	2013-05-04	2014-12-31	HHZ HHN HHE
AM16	-21.72623	46.39637	755	341	50	L4-3D	4181	CUBE	733	2013-05-03	2013-11-13	HHZ HHN HHE
AM16A	-21.71914	46.37885	733	341	50	L4-3D	4181	CUBE	733	2013-11-14	2014-12-31	HHZ HHN HHE
AM17	-22.16668	46.15255	726	341	50	L4-3D	4199	CUBE	627	2013-05-03	2014-12-31	HHZ HHN HHE
AM18	-22.57065	46.42732	638	341	50	L4-3D	4194	CUBE	734	2013-05-02	2014-12-31	HHZ HHN HHE
AM19	-22.69986	46.14377	1038	341	50	L4-3D	4198	CUBE	628	2013-05-02	2014-12-31	HHZ HHN HHE
AM20	-22.30282	45.68227	1088	341	50	L4-3D	4192	CUBE	736	2013-04-30	2014-12-31	HHZ HHN HHE
AM21	-22.61366	45.39588	800	341	50	L4-3D	4193	CUBE	737	2013-04-29	2014-12-31	HHZ HHN HHE
AM22	-22.64377	45.70106	929	341	50	L4-3D	4185	CUBE	633	2013-04-30	2014-12-31	HHZ HHN HHE
AM23	-22.94958	46.13974	1030	341	50	L4-3D	4196	CUBE	629	2013-05-02	2014-12-31	HHZ HHN HHE
MS01	-23.41386	43.75462	12	341	100	CMG-3ESP/60	GC259	PS6-SC	3222	2012-04-30	2013-04-29	HHZ HHN HHE
MS01	-23.41386	43.75462	12	341	50	L4-3D	4187	CUBE	630	2013-04-29	2014-12-31	HHZ HHN HHE
MS02	-23.34335	43.89449	166	341	50	L4-3D	4186	CUBE	632	2013-04-29	2014-12-31	HHZ HHN HHE
MS02	-23.34335	43.89449	166	341	100	CMG-3ESP/60	GC257	PS6-SC	3221	2012-04-30	2013-04-28	HHZ HHN HHE
MS03	-23.23817	44.02398	326	341	50	L4-3D	4184	CUBE	631	2013-04-29	2014-12-31	HHZ HHN HHE
MS03	-23.23817	44.02398	326	341	100	CMG-3ESP/60	GC244	PS6-SC	3216	2012-04-29	2013-04-28	HHZ HHN HHE
MS04	-23.10502	44.21986	439	341	100	Trillium-240	GC633	PS6-SC	3252	2012-05-03	2014-12-31	HHZ HHN HHE
MS05	-22.90606	44.46386	421	341	100	CMG-3ESP/60	GC254	PS6-SC	3246	2012-05-04	2012-09-29	HHZ HHN HHE
MS05	-22.90606	44.46386	421	341	100	CMG-3ESP/60	GC260	PS6-SC	3246	2012-09-30	2013-04-25	HHZ HHN HHE
MS05	-22.90606	44.46386	421	341	100	CMG-3ESP/60	GC238	PS6-SC	3240	2013-04-26	2014-12-31	HHZ HHN HHE
MS06	-22.88615	44.69135	820	341	100	CMG-3ESP/60	GC238	PS6-SC	3226	2012-05-05	2014-12-31	HHZ HHN HHE
MS06A	-22.8271	44.73273	970	341	100	CMG-3ESP/60	GC252	PS6-SC	3226	2013-04-26	2014-12-31	HHZ HHN HHE
MS07	-22.81237	44.82891	663	341	100	Trillium-240	GC632	PS6-SC	3250	2012-04-28	2014-12-31	HHZ HHN HHE
MS08	-22.7548	45.11313	855	341	100	CMG-3ESP/60	GC245	PS6-SC	3249	2012-05-02	2014-12-31	HHZ HHN HHE
MS09	-22.48263	45.39815	723	341	100	CMG-3ESP/60	GC240	PS6-SC	3220	2012-05-04	2014-12-31	HHZ HHN HHE
MS10	-22.47355	45.56681	972	341	100	CMG-3ESP/60	GC249	PS6-SC	3241	2012-05-04	2014-12-31	HHZ HHN HHE
MS11	-22.5197	45.72152	961	341	100	Trillium-240	GC630	PS6-SC	3251	2012-05-03	2014-12-31	HHZ HHN HHE
MS12	-22.43738	45.91504	1038	341	100	CMG-3ESP/60	GC256	PS6-SC	3244	2012-05-03	2014-12-31	HHZ HHN HHE
MS13	-22.35751	46.0879	732	341	100	CMG-3ESP/60	GC255	PS6-SC	3242	2012-05-01	2014-12-31	HHZ HHN HHE
MS14	-22.29951	46.25156	721	341	100	CMG-3ESP/60	GC243	PS6-SC	3219	2012-05-01	2014-12-31	HHZ HHN HHE
MS15	-22.08547	46.40907	965	341	100	CMG-3ESP/60	GC250	PS6-SC	3225	2012-04-30	2014-01-11	HHZ HHN HHE
MS15	-22.08547	46.40907	965	341	100	CMG-3ESP/60	GC250	PS6-SC	3246	2014-01-12	2014-12-31	HHZ HHN HHE
MS16	-21.93573	46.543	772	341	100	CMG-3ESP/60	GC248	PS6-SC	3217	2012-05-01	2014-12-31	HHZ HHN HHE
MS17	-21.78999	46.92598	963	341	50	L4-3D	4189	CUBE	634	2013-04-27	2014-12-31	HHZ HHN HHE
MS17	-21.78999	46.92598	963	341	100	CMG-3ESP/60	GC252	PS6-SC	3247	2012-04-30	2013-04-26	HHZ HHN HHE
MS18	-21.59757	46.99488	1200	341	100	CMG-3ESP/60	GC260	PS6-SC	3248	2012-04-30	2014-12-31	HHZ HHN HHE
MS18A	-21.59754	46.99477	1200	341	100	CMG-3ESP/60	GC257	PS6-SC	3247	2013-05-04	2014-12-31	HHZ HHN HHE
MS19	-21.40929	47.10285	1140	341	100	CMG-3ESP/60	GC239	PS6-SC	3245	2012-05-07	2014-12-31	HHZ HHN HHE
MS20	-21.33165	47.27146	1126	341	100	Trillium-240	GC634	PS6-SC	3253	2012-05-08	2014-12-31	HHZ HHN HHE
MS21	-21.23891	47.38246	1135	341	100	CMG-3ESP/60	GC253	PS6-SC	3218	2012-05-08	2014-12-31	HHZ HHN HHE
MS22	-21.33823	47.61607	463	341	50	L4-3D	400289	CUBE	731	2013-05-05	2014-12-31	HHZ HHN HHE
MS22	-21.33823	47.61607	463	341	100	CMG-3ESP/60	GC247	PS6-SC	3240	2012-04-26	2013-05-05	HHZ HHN HHE
MS23	-21.35424	47.77802	254	341	100	CMG-3ESP/60	GC251	PS6-SC	3215	2012-04-27	2014-12-31	HHZ HHN HHE
MS24	-21.42538	48.03929	197	341	100	Trillium-240	GC631	PS6-SC	3254	2012-04-28	2014-12-31	HHZ HHN HHE
MS25	-21.27671	48.17101	76	341	100	CMG-3ESP/60	GC242	PS6-SC	3243	2012-04-28	2014-12-31	HHZ HHN HHE
MS25A	-21.2876	48.1858	109	341	50	L4-3D	3054	CUBE	726	2013-05-08	2014-12-31	HHZ HHN HHE

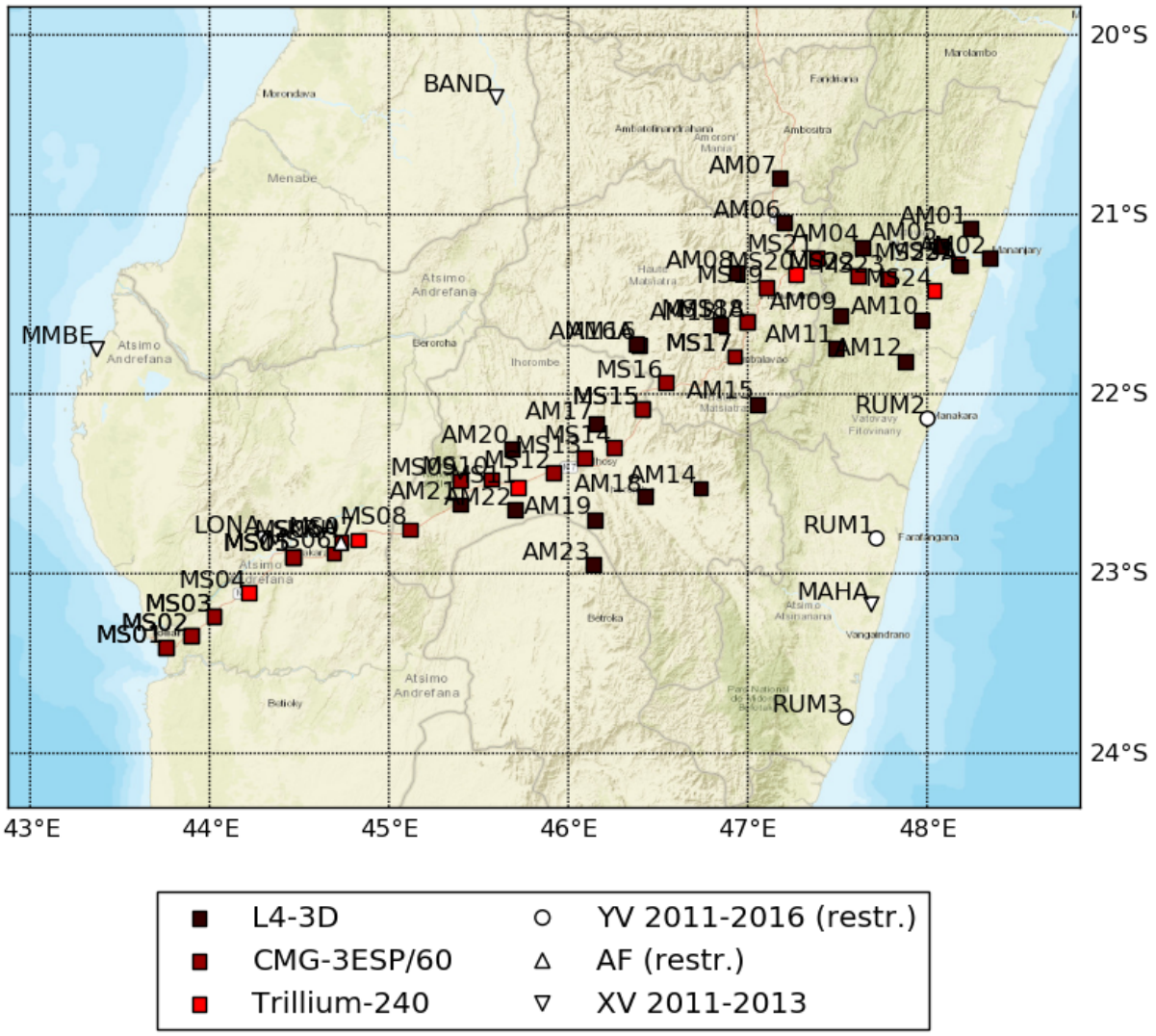

Fig. 1: Station distribution in experiment (red symbols). If present, white-filled symbols show permanent stations and other temporary experiments archived at EIDA or IRIS-DMC, whose activity period overlapped at least partially with the time of the experiment. If present, open symbols show station sites which were no longer active at the time of the experiment, e.g. prior temporary experiments.

Fig. 2: Typical station installation - sensor, data logger and battery are buried for protection against daily temperature cycle and vandalism (picture shows MS04).

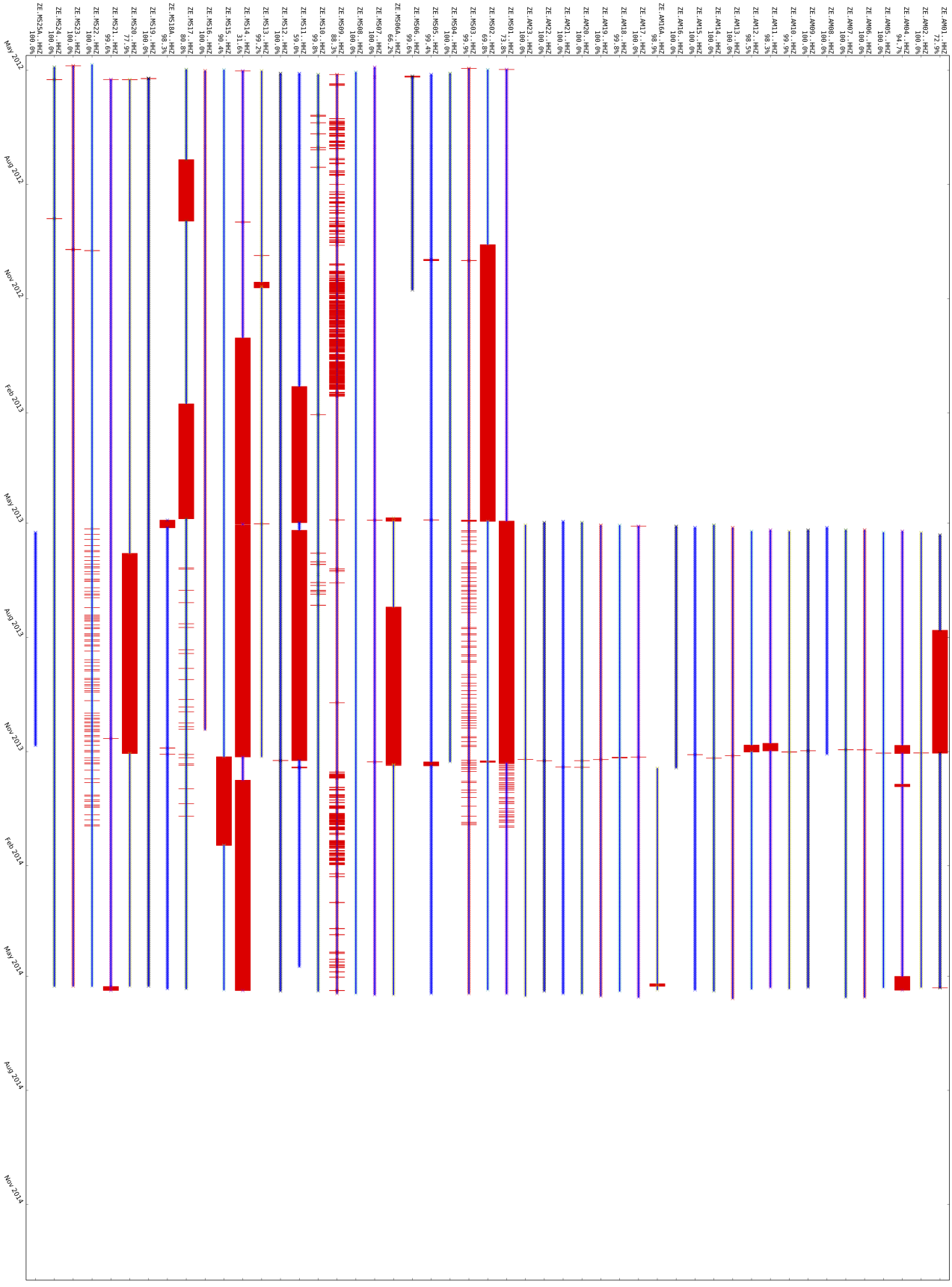

Fig. 3: Overview of uptimes of all stations generated with *obspy-scan*

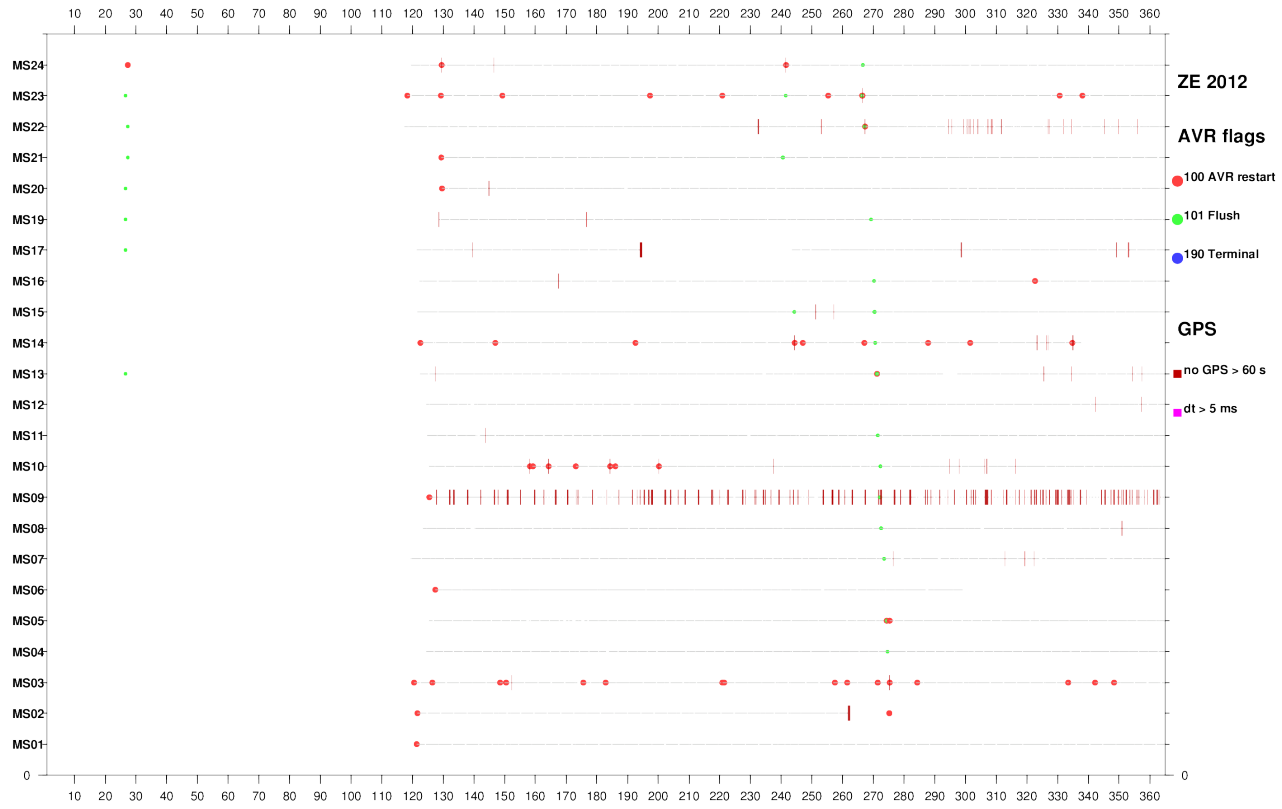

Fig. 4: Status report of EDL stations for 2012 showing restart events (AVR), service times (flush) and potential GPS problems (vertical bars indicating temporary gaps in GPS coverage). Generally even station with a large number number of GPS gaps will provide reliable timing as long as at least one GPS lock per day is picked up.

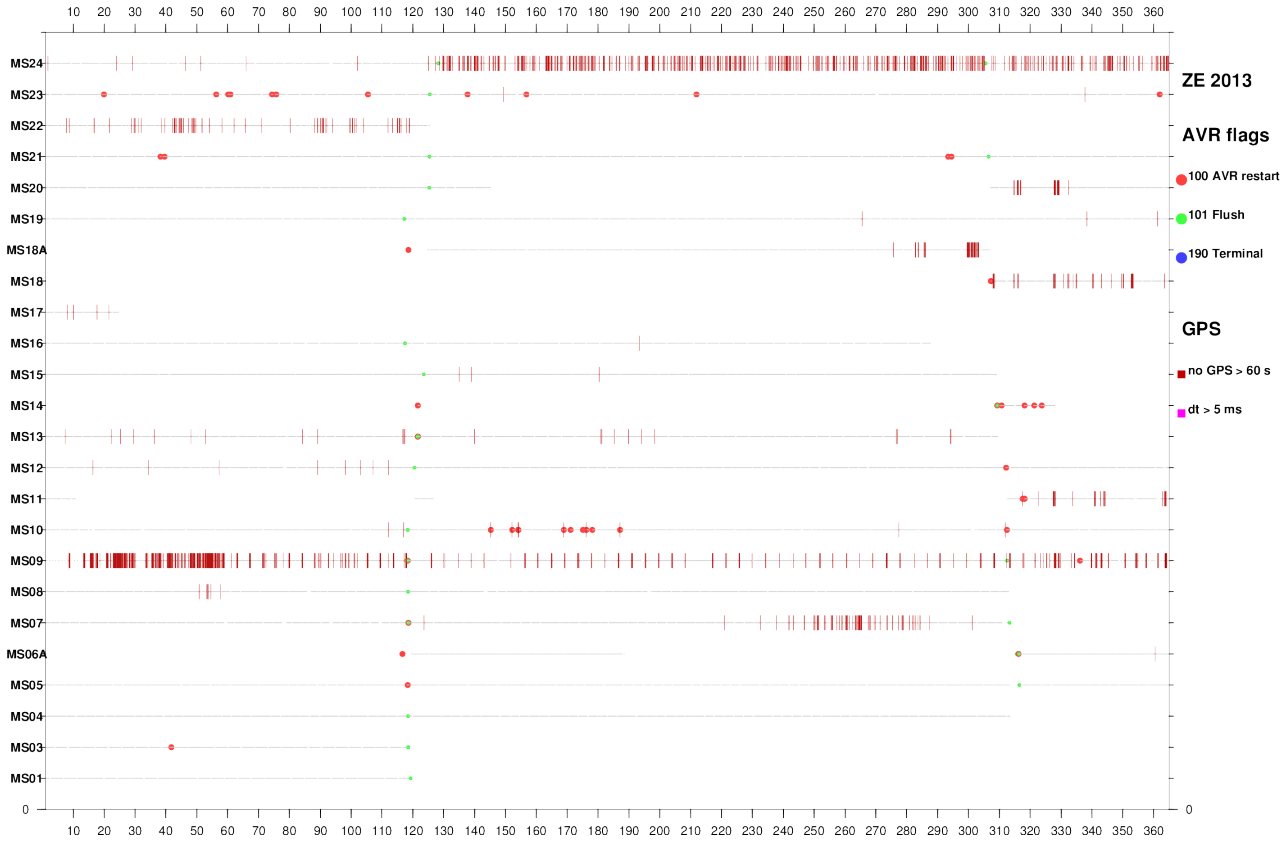

Fig. 5: (as Fig. 5) but for 2013.

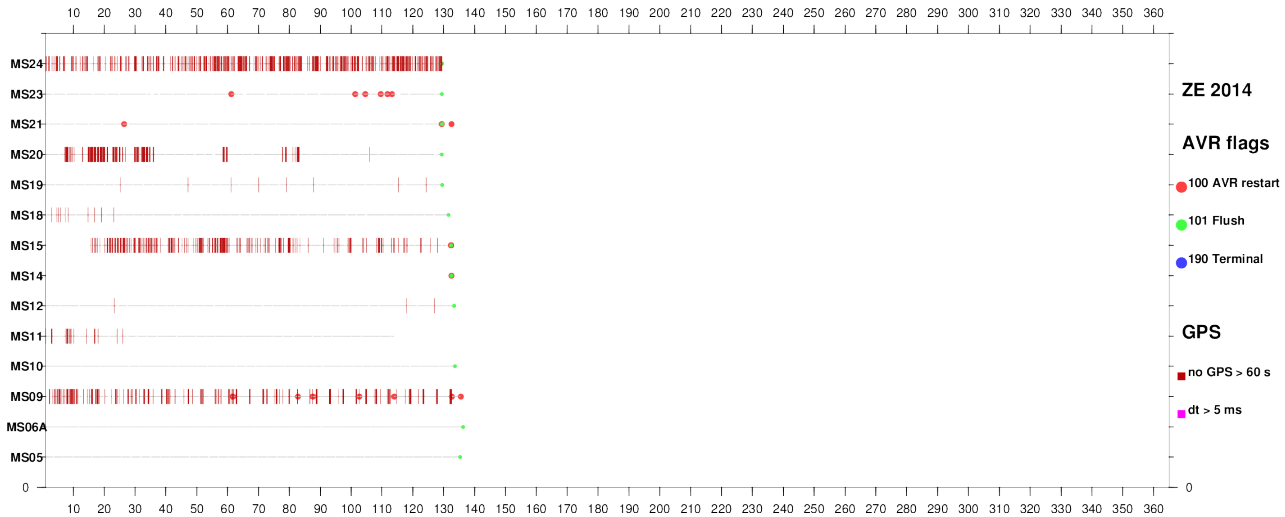

Fig. 6: (as Fig. 4) but for 2014.

HHZ HHN HHE

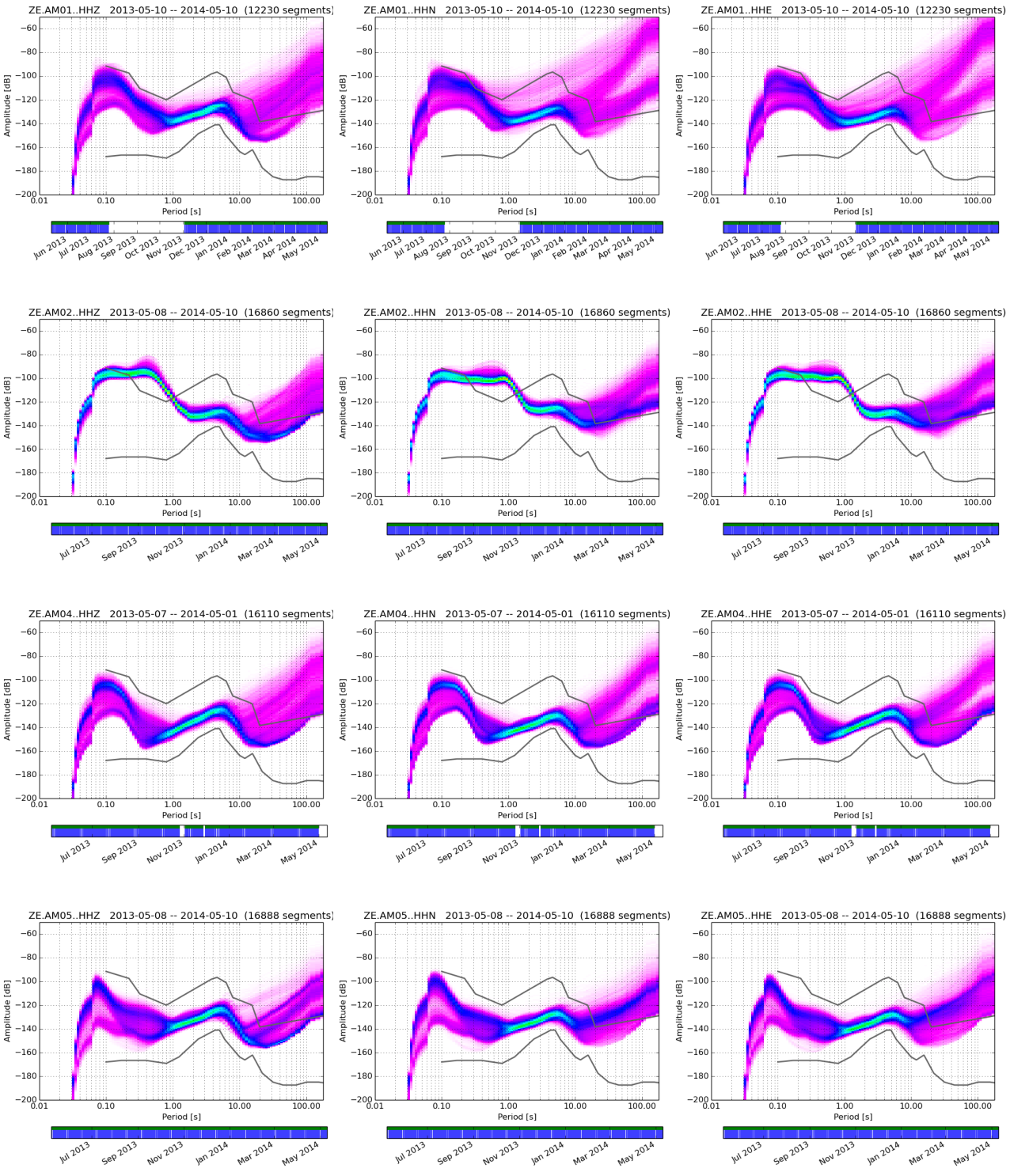

Fig. 7 – continued on next page

Continued from previous page

HHZ HHN HHE

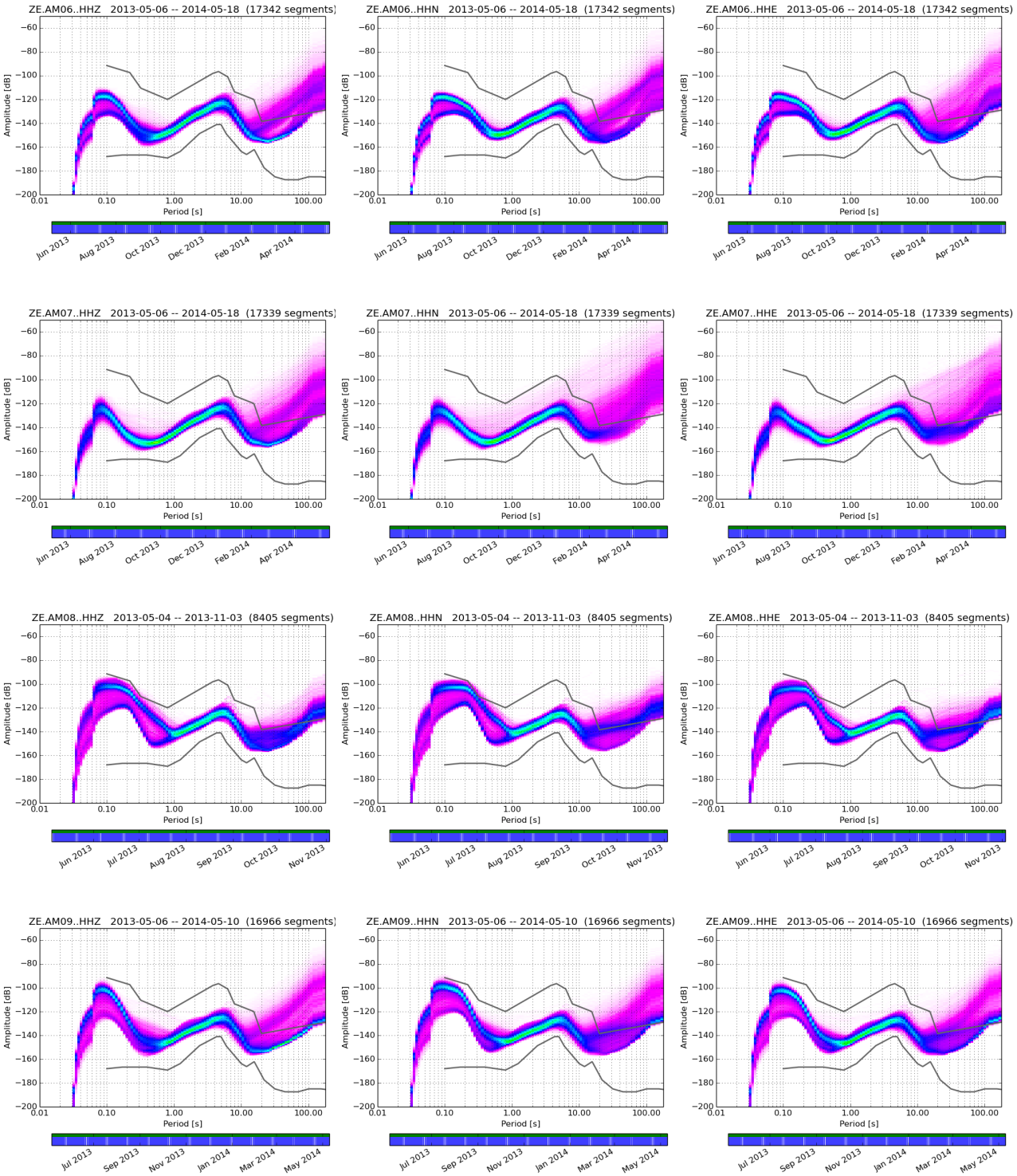

Fig. 7 – continued on next page

Continued from previous page

HHZ HHN HHE

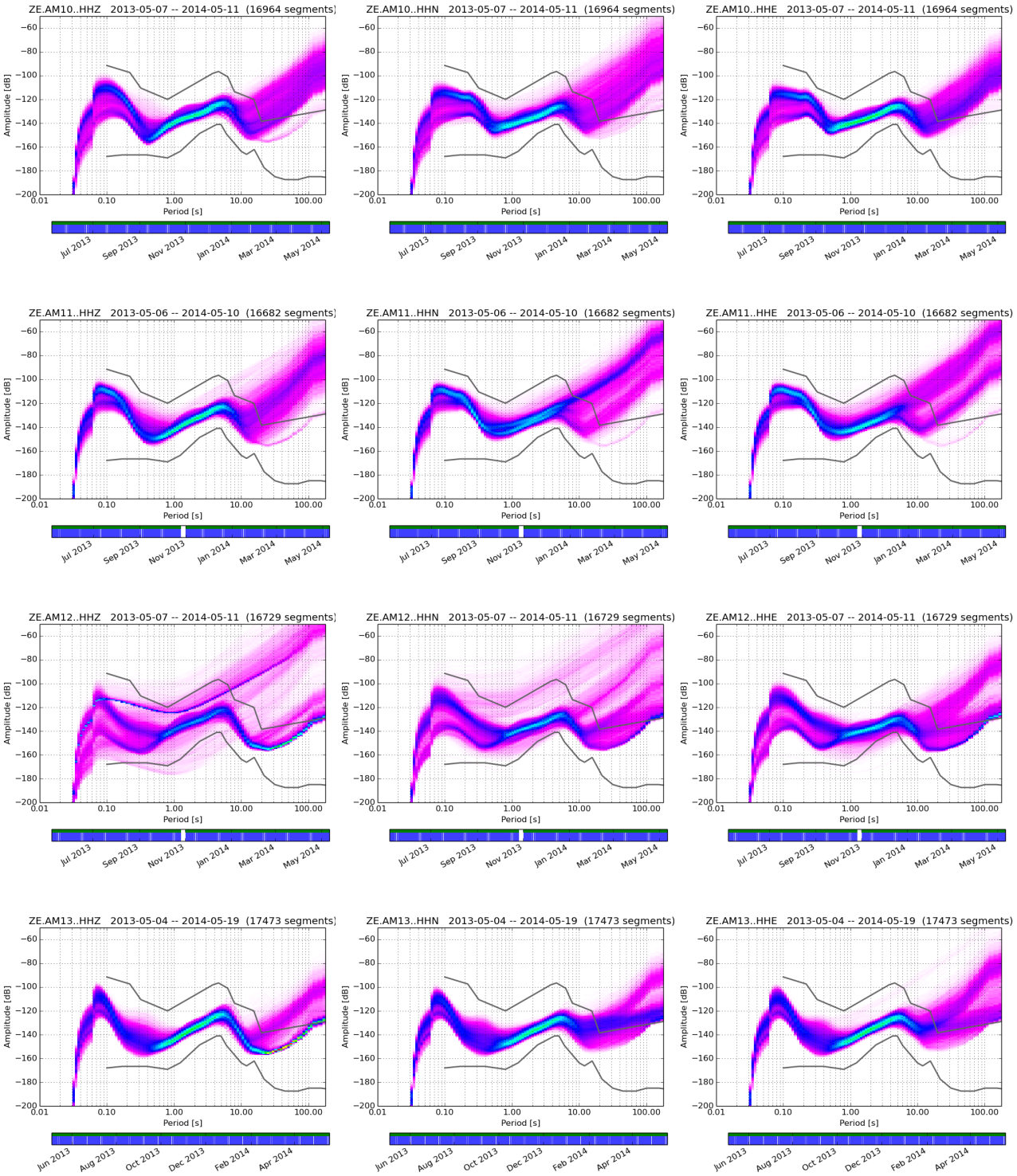

Fig. 7 – continued on next page

Continued from previous page

HHZ HHN HHE

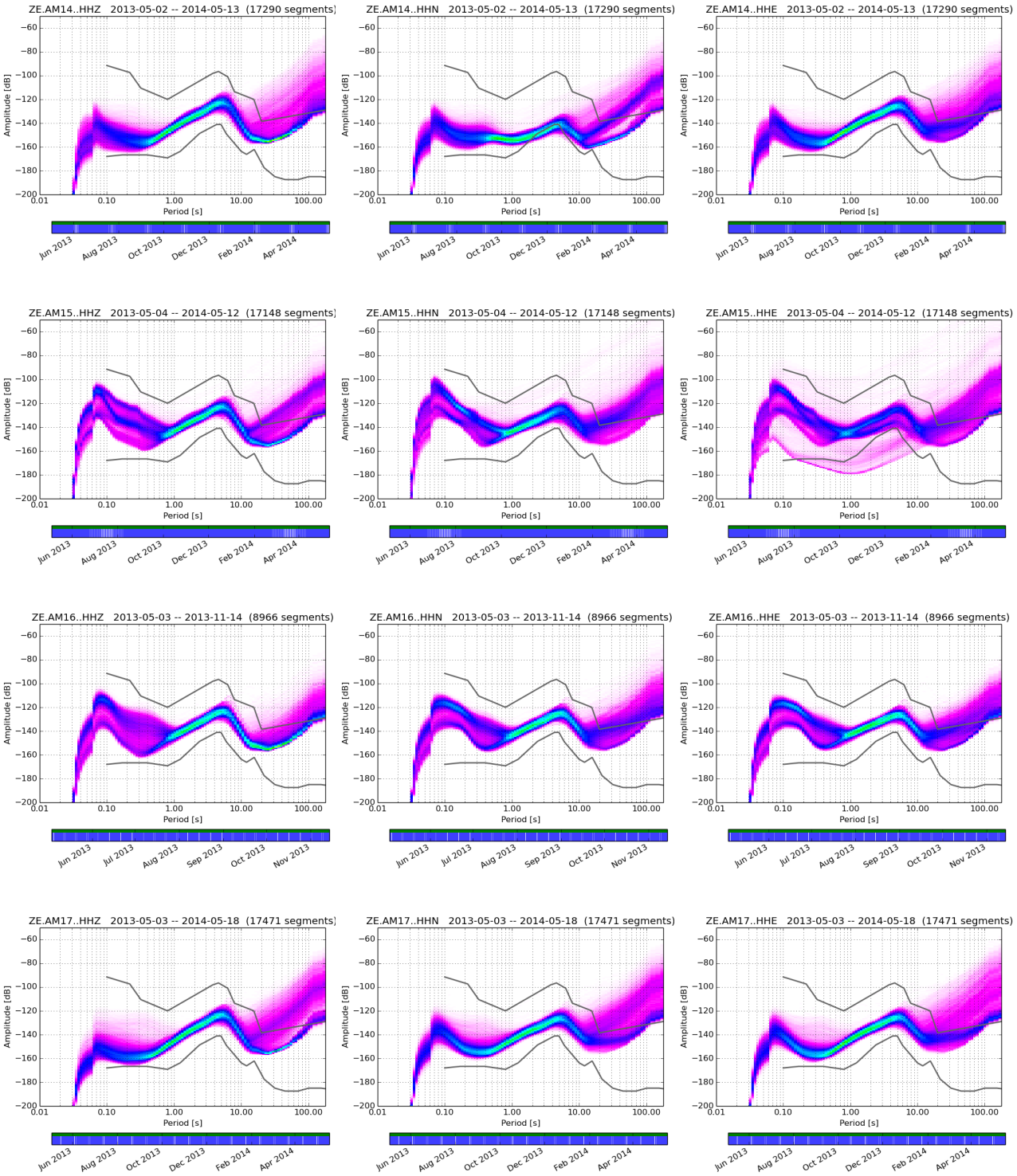

Fig. 7 – continued on next page

Continued from previous page

HHZ HHN HHE

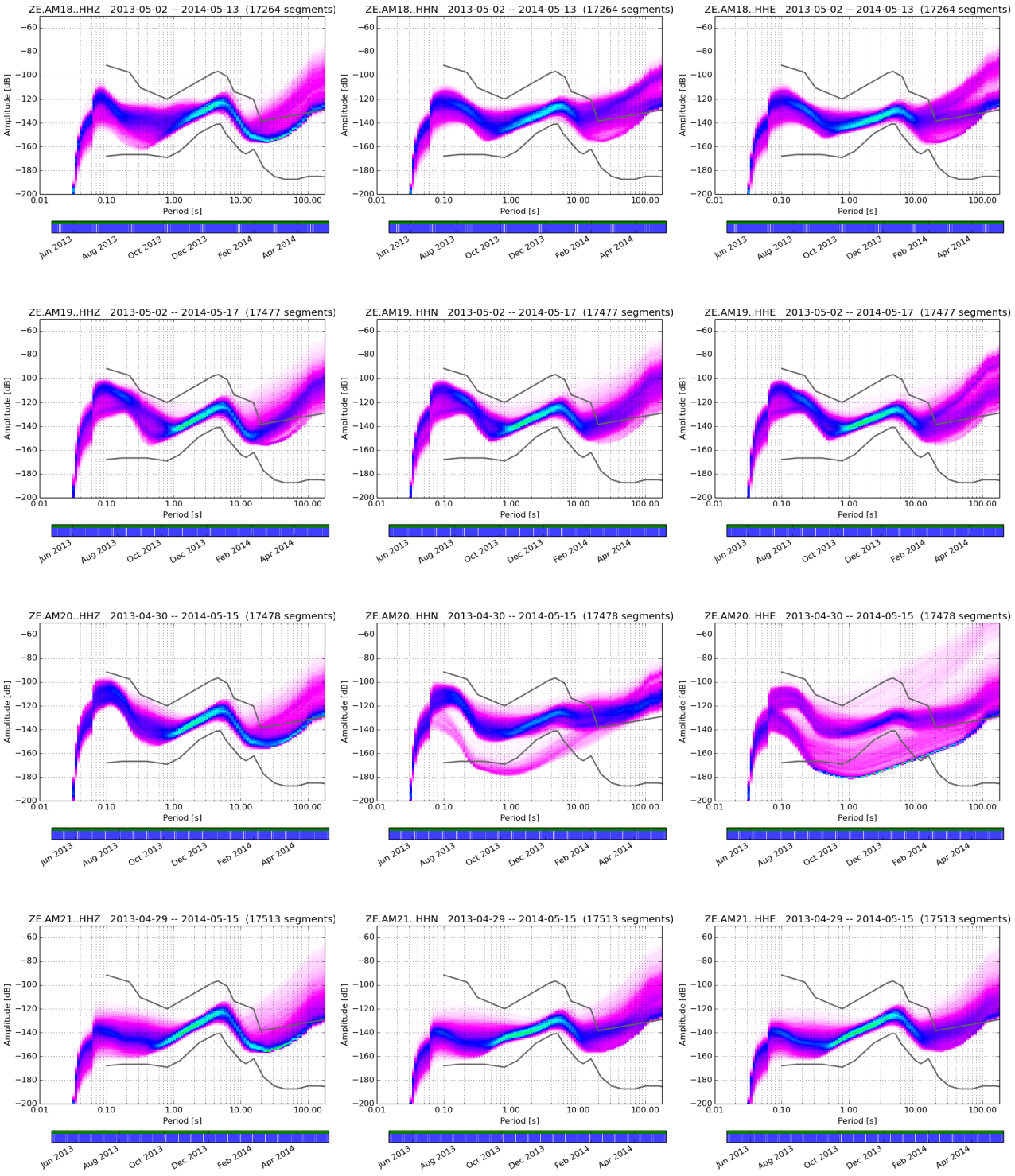

Fig. 7 – continued on next page

Continued from previous page

HHZ HHN HHE

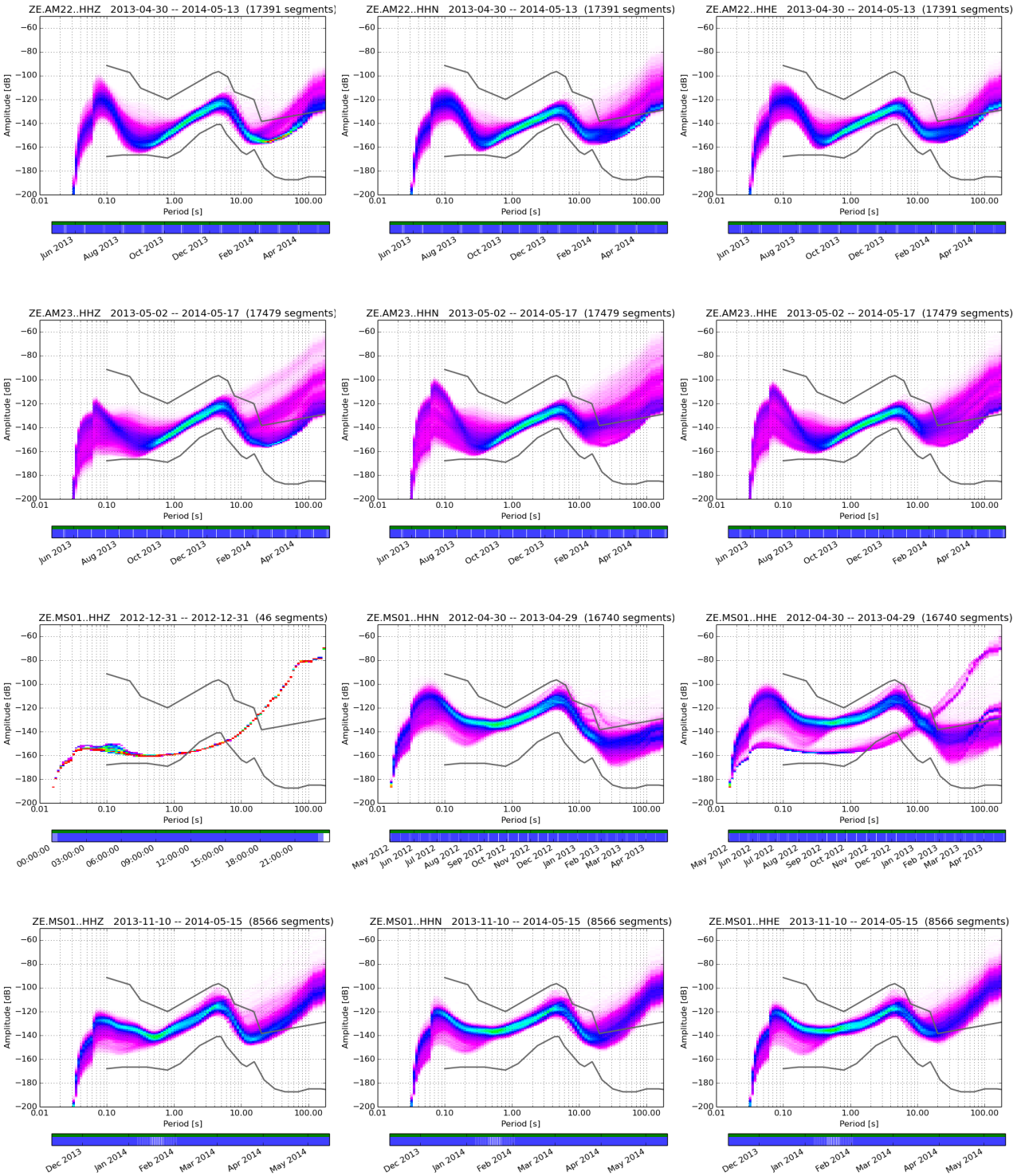

Fig. 7 – continued on next page

Continued from previous page

HHZ HHN HHE

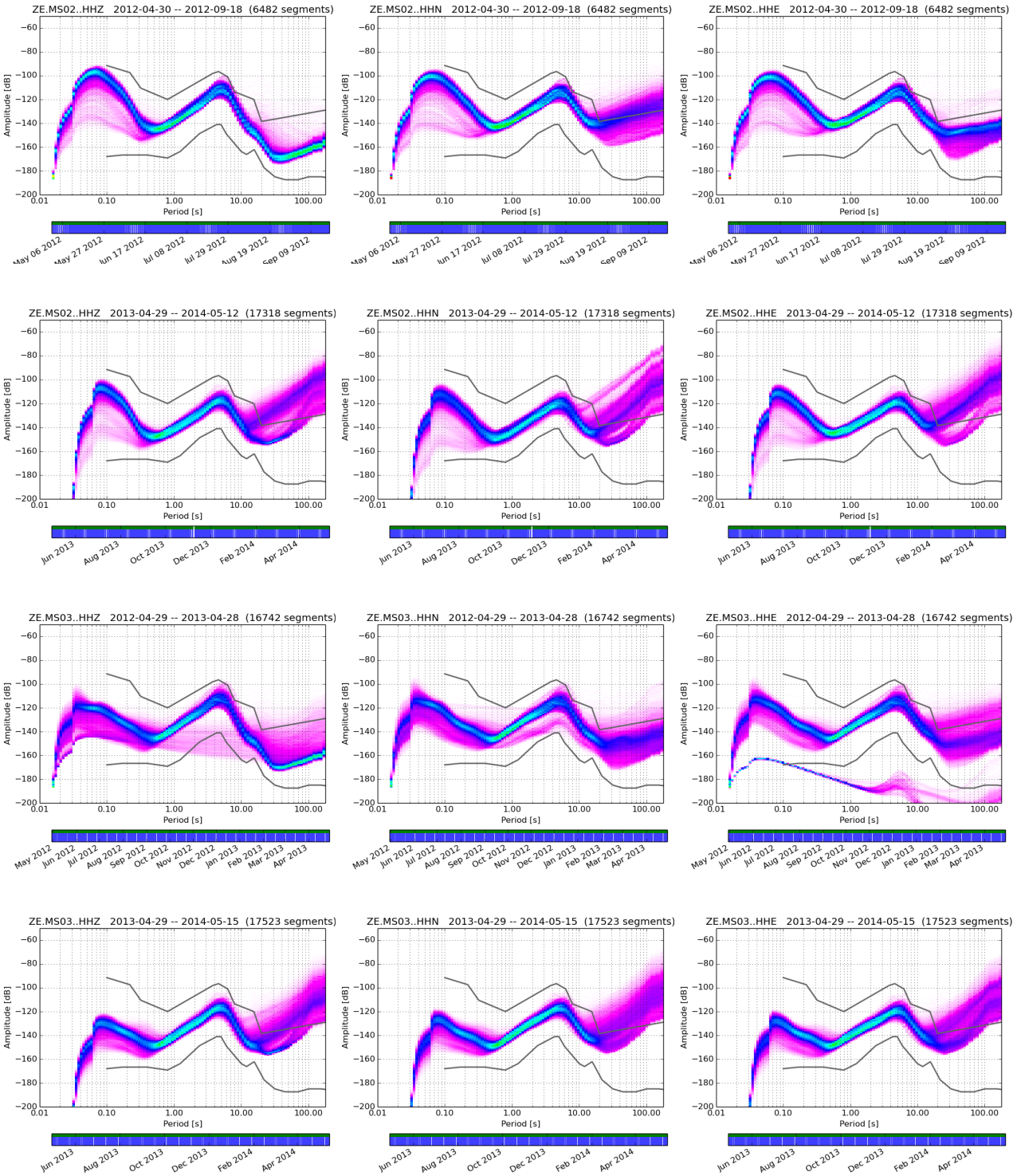

Fig. 7 – continued on next page

Continued from previous page

HHZ HHN HHE

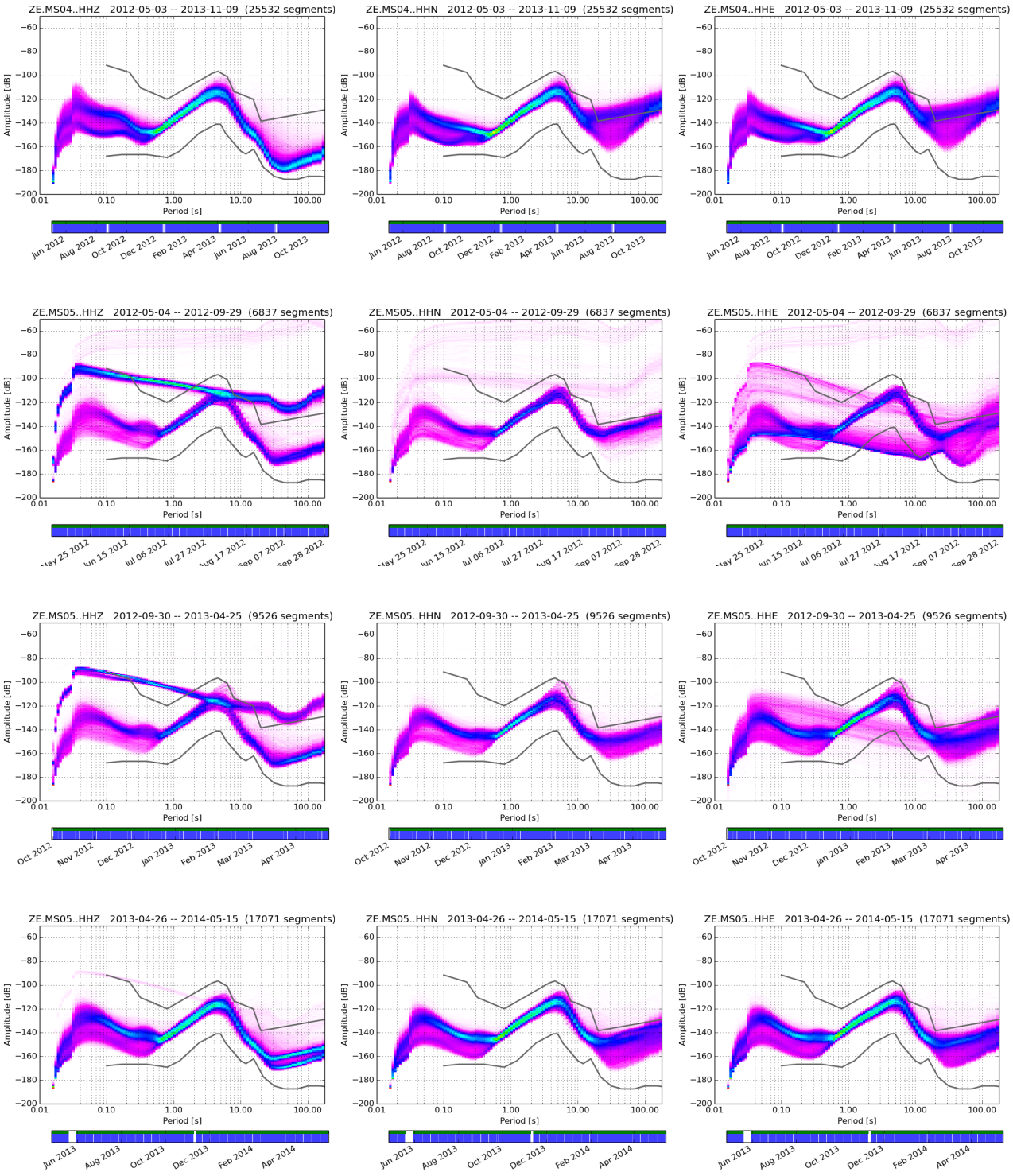

Fig. 7 – continued on next page

Continued from previous page

HHZ HHN HHE

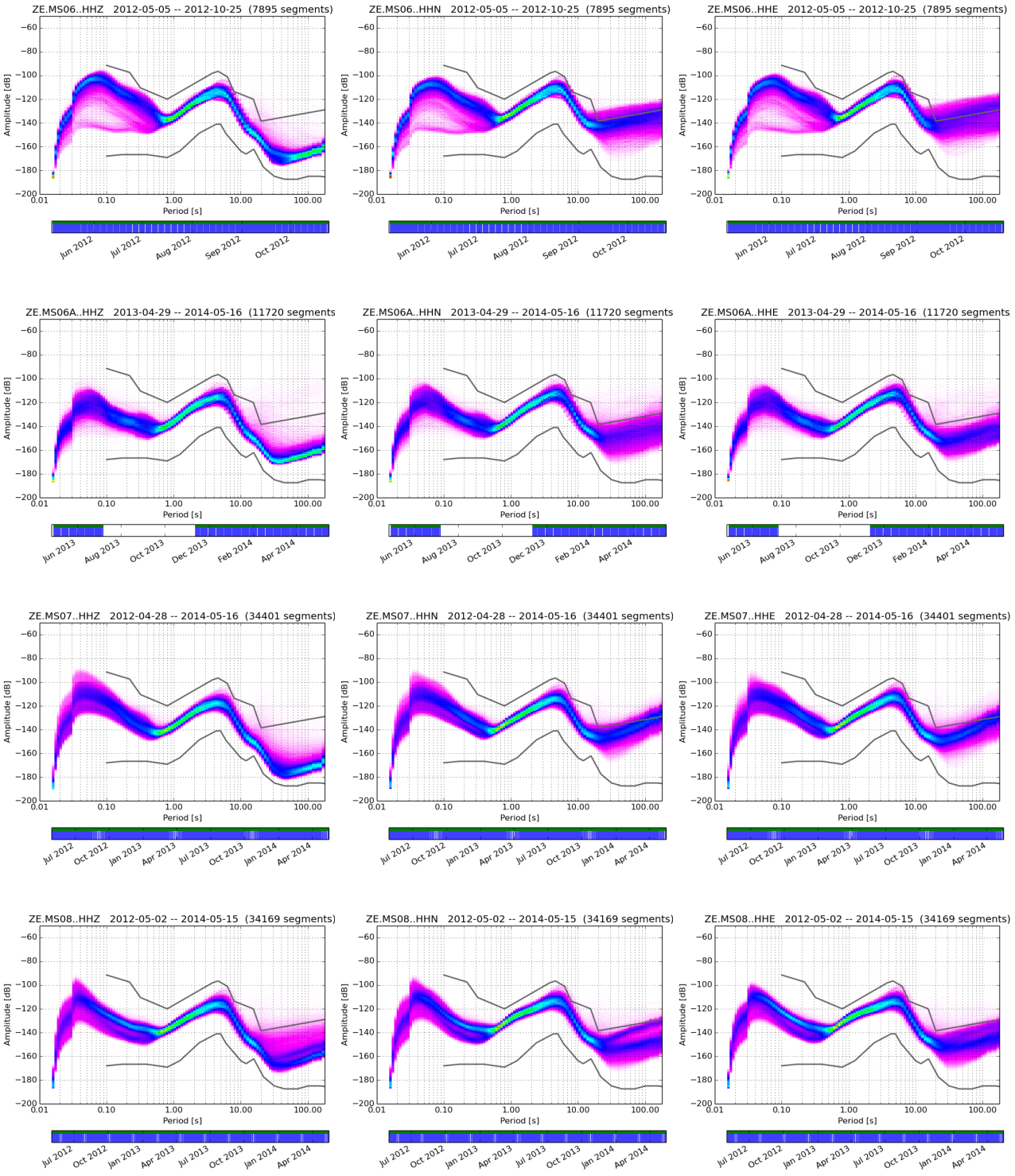

Fig. 7 – continued on next page

Continued from previous page

HHZ HHN HHE

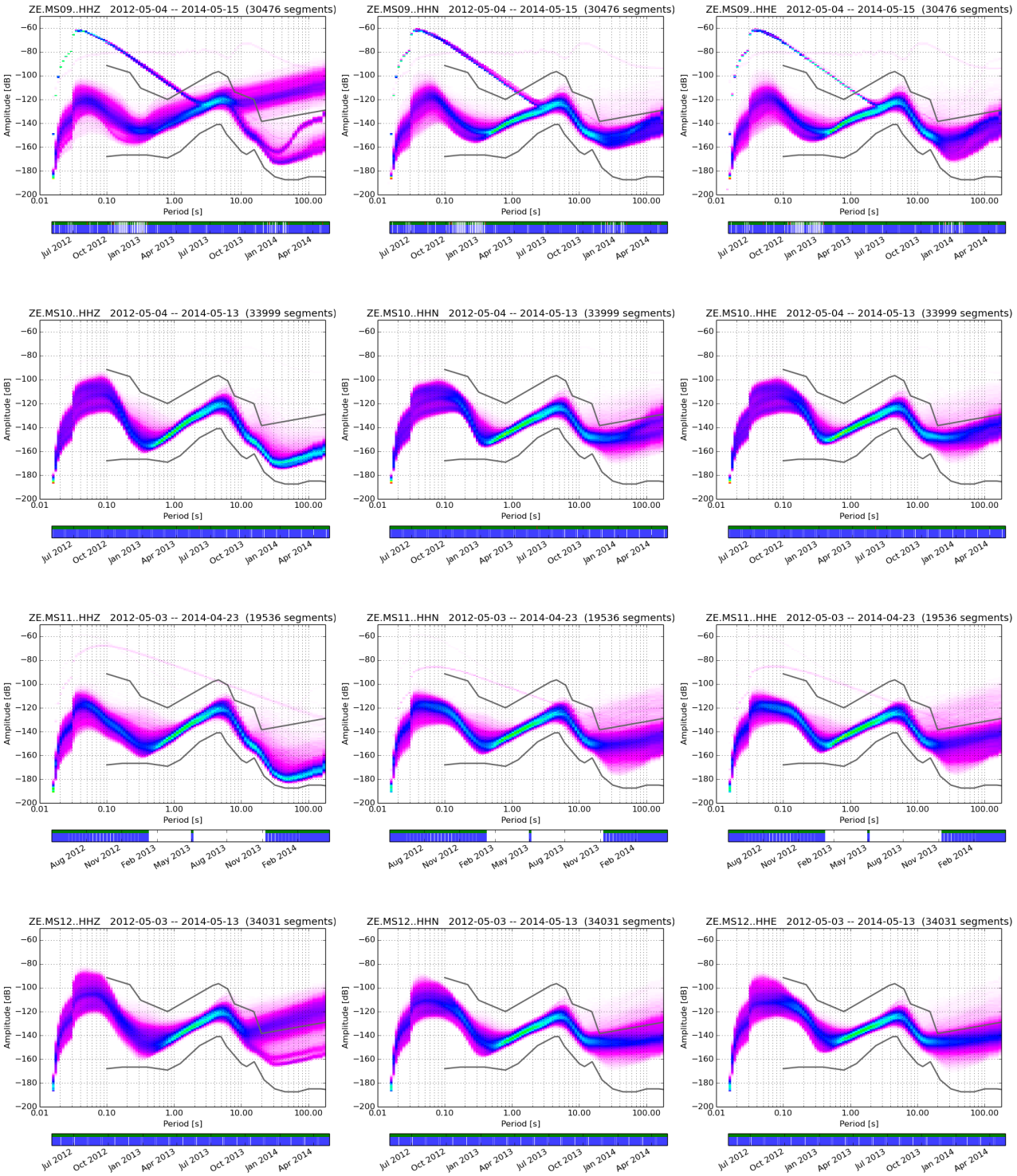

Fig. 7 – continued on next page

Continued from previous page

HHZ HHN HHE

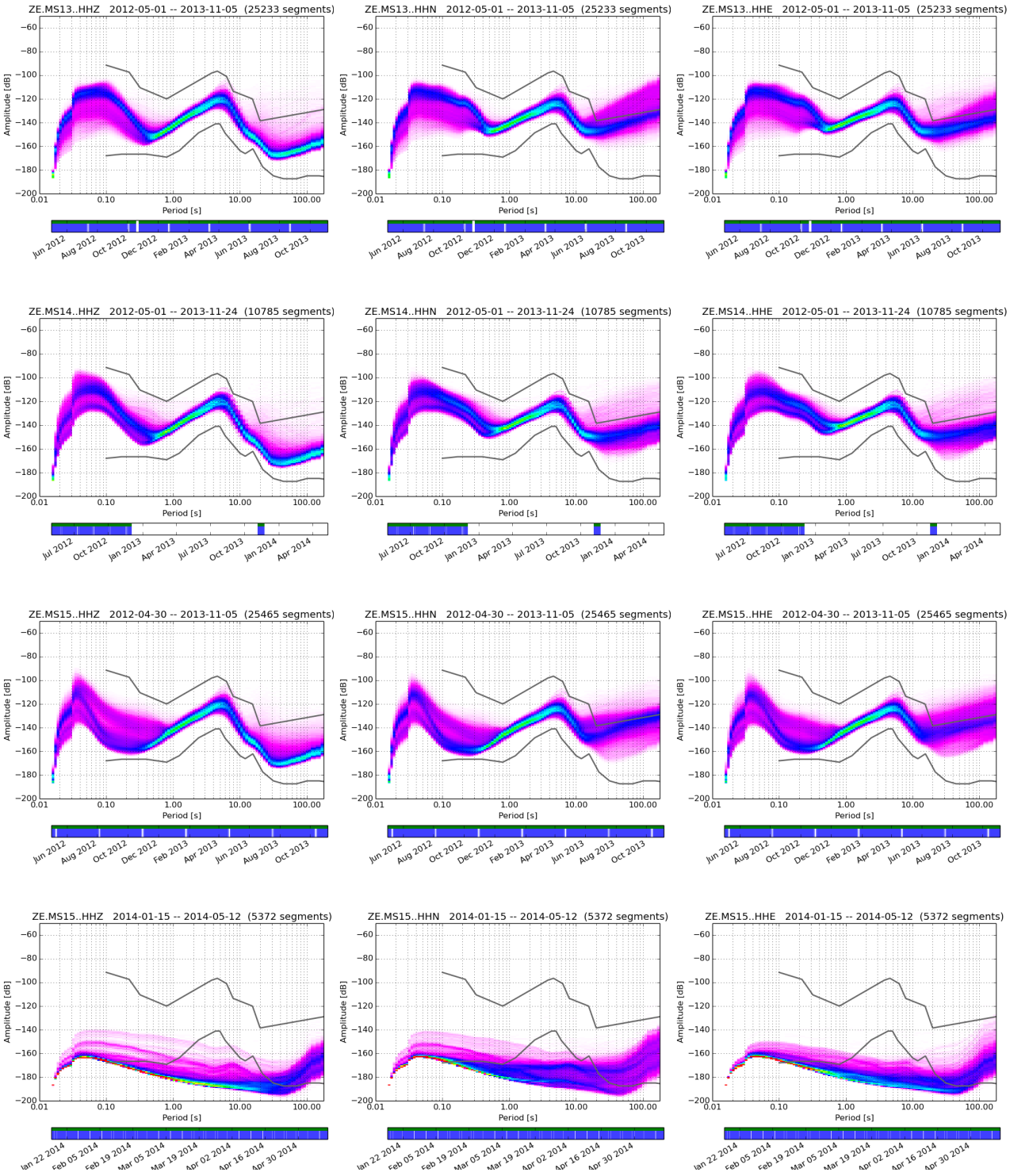

Fig. 7 – continued on next page

Continued from previous page

HHZ HHN HHE

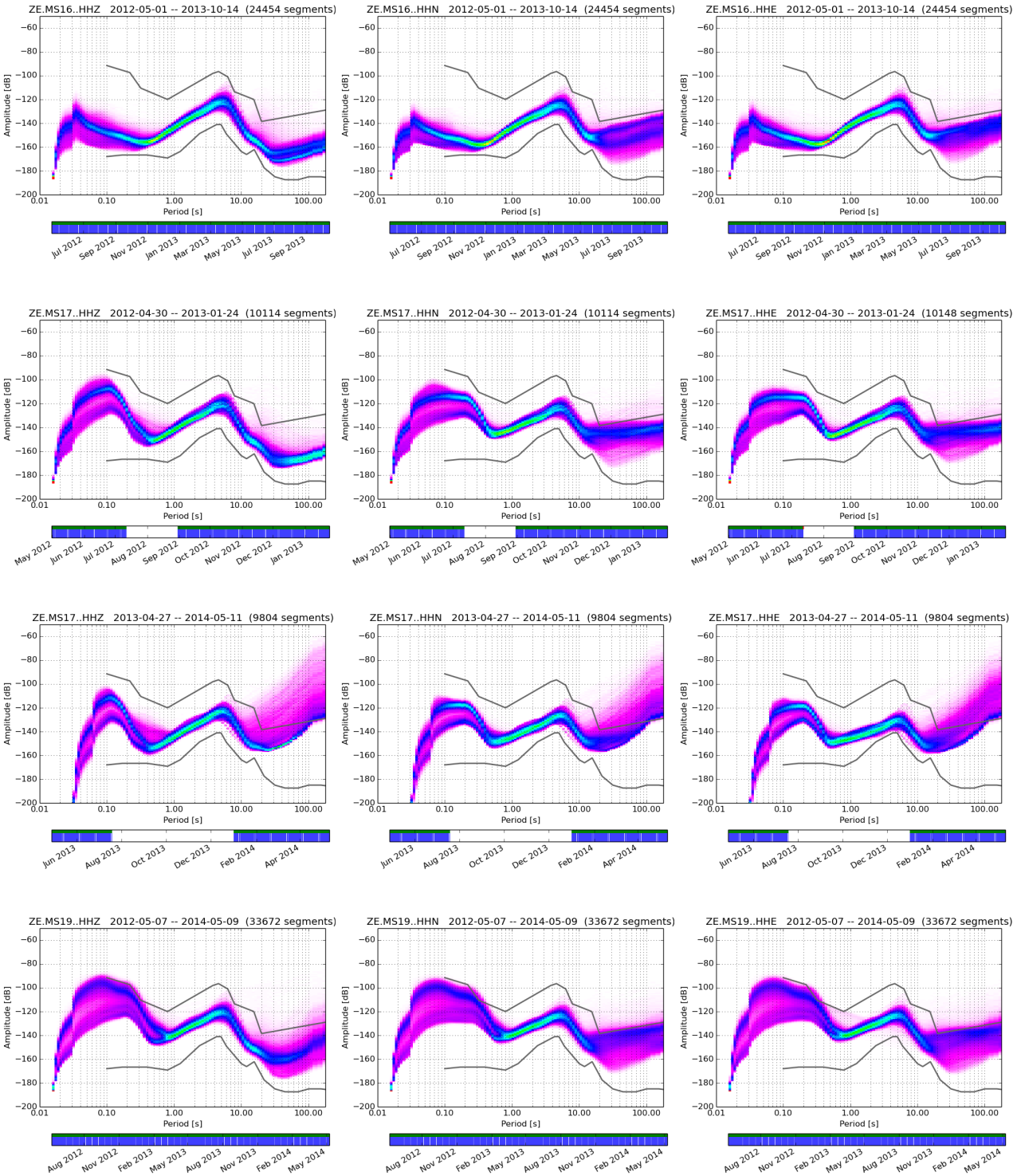

Fig. 7 – continued on next page

Continued from previous page

HHZ HHN HHE

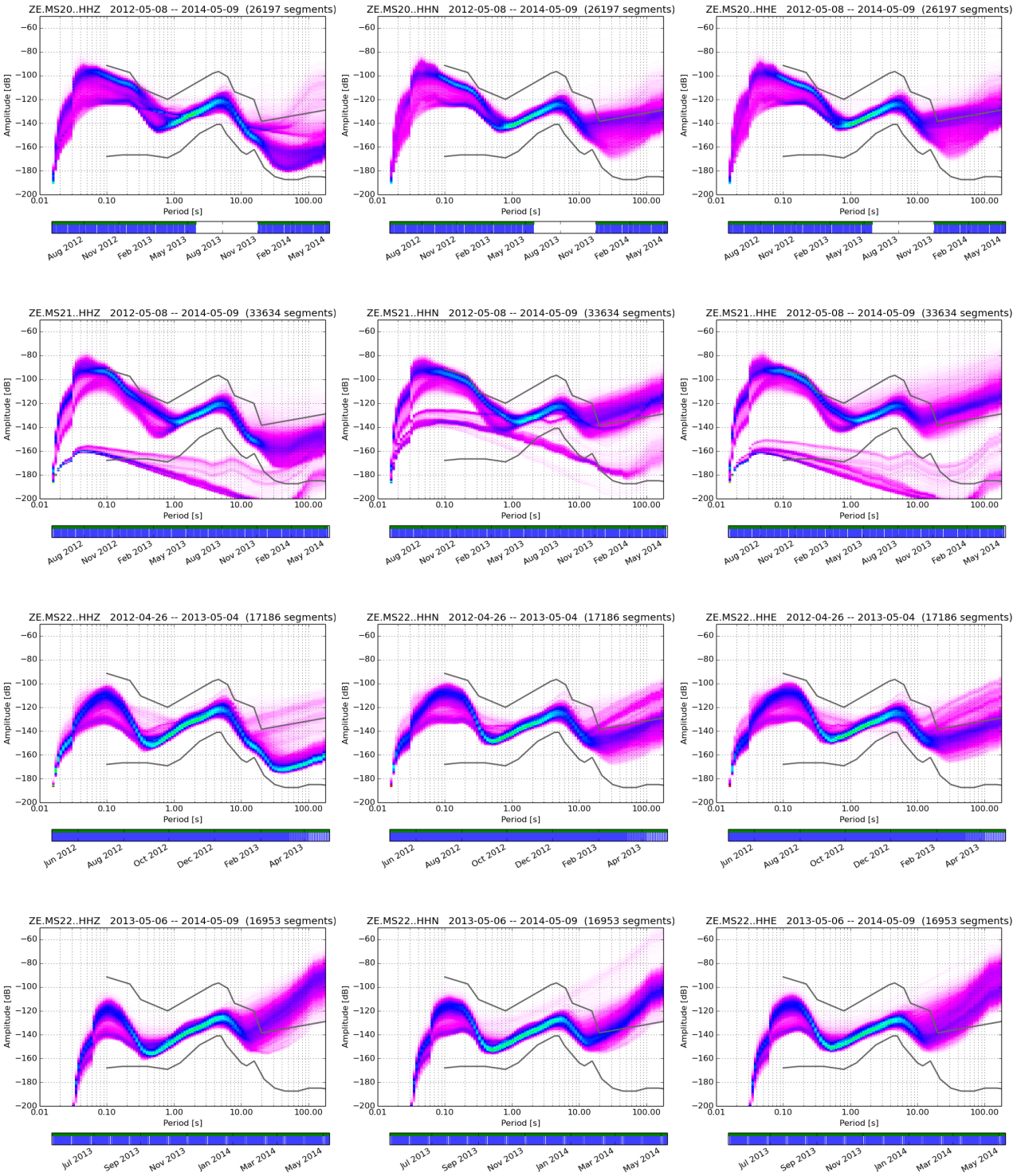

Fig. 7 – continued on next page

Continued from previous page

HHZ HHN HHE

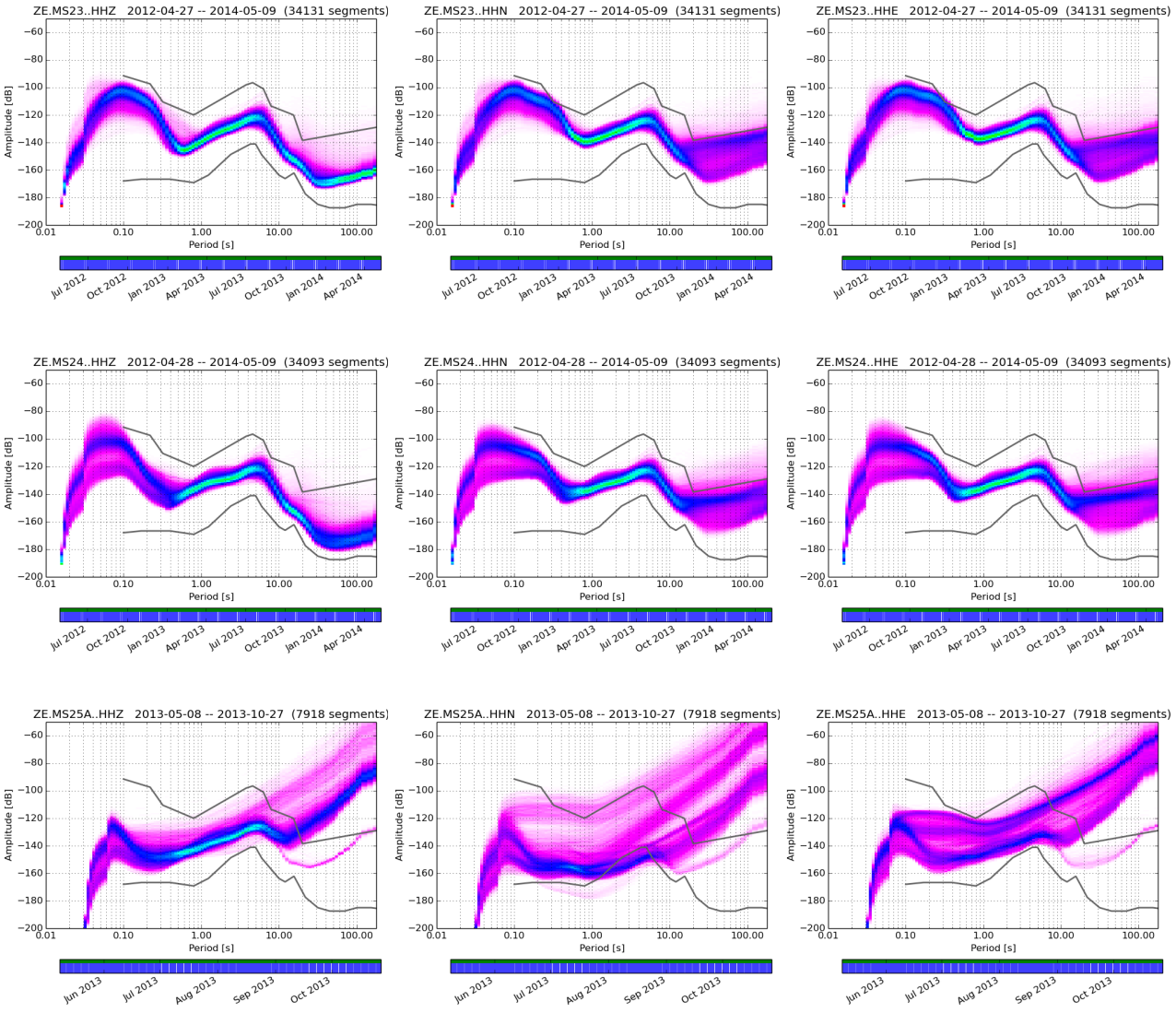

Fig. 7: Noise probability density functions for all stations for database holdings

References

[RYBERG14] Trond Ryberg. Cube timing errors introduced by long periods without gps reception, 2014. URL http://www.gfz-potsdam.de/fileadmin/gfz/sec22/pdf_doc/GIPP/cube/Cube_timing_errors_no_gps.pdf

ISSN 2190-7110